Acetylation of H2A.Z is a key epigenetic modification associated with gene deregulation and epigenetic remodeling in cancer

Fátima Valdés-Mora,[1] Jenny Z. Song,[1] Aaron L. Statham,[1] Dario Strbenac,[1] Mark D. Robinson,[1,2] Shalima S. Nair,[1] Kate I. Patterson,[1] David J. Tremethick,[3] Clare Stirzaker,[1] and Susan J. Clark[1,4,5]

[1]*Epigenetics Laboratory, Cancer Research Program, Garvan Institute of Medical Research, Sydney 2010, New South Wales, Australia;* [2]*Bioinformatics Division, Walter and Eliza Hall Institute of Medical Research, Parkville, Melbourne 3050, Victoria, Australia;* [3]*Chromatin and Transcriptional Regulation Group, John Curtin School of Medical Research, Australian National University, Canberra 2000, Australian Capital Territory, Australia;* [4]*St. Vincent's Clinical School, Faculty of Medicine, University of New South Wales, Sydney 2052, New South Wales, Australia*

Histone H2A.Z (H2A.Z) is an evolutionarily conserved H2A variant implicated in the regulation of gene expression; however, its role in transcriptional deregulation in cancer remains poorly understood. Using genome-wide studies, we investigated the role of promoter-associated H2A.Z and acetylated H2A.Z (acH2A.Z) in gene deregulation and its relationship with DNA methylation and H3K27me3 in prostate cancer. Our results reconcile the conflicting reports of positive and negative roles for histone H2A.Z and gene expression states. We find that H2A.Z is enriched in a bimodal distribution at nucleosomes, surrounding the transcription start sites (TSSs) of both active and poised gene promoters. In addition, H2A.Z spreads across the entire promoter of inactive genes in a deacetylated state. In contrast, acH2A.Z is only localized at the TSSs of active genes. Gene deregulation in cancer is also associated with a reorganization of acH2A.Z and H2A.Z nucleosome occupancy across the promoter region and TSS of genes. Notably, in cancer cells we find that a gain of acH2A.Z at the TSS occurs with an overall decrease of H2A.Z levels, in concert with oncogene activation. Furthermore, deacetylation of H2A.Z at TSSs is increased with silencing of tumor suppressor genes. We also demonstrate that acH2A.Z anti-correlates with promoter H3K27me3 and DNA methylation. We show for the first time, that acetylation of H2A.Z is a key modification associated with gene activity in normal cells and epigenetic gene deregulation in tumorigenesis.

[Supplemental material is available for this article.]

Epigenetics involves the understanding of chromatin structure and its impact on the regulation of gene expression. Epigenetic mechanisms that modify chromatin structure include DNA methylation, histone post-synthetic modifications, nucleosome positioning, incorporation of histone variants into nucleosomes and expression of noncoding RNAs. The basic repeating unit of chromatin is the nucleosome, a particle consisting of an octamer of core histones (two copies each of histones H2A, H2B, H3, and H4), around which ~146 bp of DNA is wrapped (Sharma et al. 2010). Both the modification of histones and incorporation of histone variants into nucleosomes have been described to modulate chromatin structure (Kamakaka and Biggins 2005; Campos and Reinberg 2009). H2A.Z is an evolutionary conserved variant of the canonical histone H2A (H2A), which shares only ~60% sequence identity with major H2A, and is required for viability in metazoans, suggesting a unique function (Faast et al. 2001; Zlatanova and Thakar 2008) In fact, H2A.Z occupancy has been involved in contrary and varying functions in different species, including both gene activation (Barski et al. 2007) and gene silencing (Gevry et al. 2007), nucleosome turnover (Santisteban et al. 2000), DNA repair (Rong 2008), heterochromatin silencing (Rangasamy et al. 2003), chromosome segregation (Rangasamy et al. 2004), progression through the cell cycle (Dhillon et al. 2006), suppression of antisense RNAs (Zofall et al. 2009), embryonic stem cell differentiation (Creyghton et al. 2008), and antagonizing DNA methylation (Zilberman et al. 2008).

Recently, ChIP and tiling microarray technologies have provided high-resolution genome-wide information that has localized H2A.Z to the promoters of many genes in several organisms including humans, which suggests a role in gene transcription (Barski et al. 2007). However, the precise function of H2A.Z in transcriptional regulation is still poorly understood and may differ between species (Guillemette and Gaudreau 2006). In human T cells, promoter enrichment of H2A.Z is often associated with actively expressing genes (Barski et al. 2007); however, independent studies show that H2A.Z can also be found at particular promoters of inducible genes, where it functions to repress expression (Gevry et al. 2007; Sutcliffe et al. 2009). Thus, deposition of H2A.Z at the 5′ end of genes may act to set up chromatin architecture that is compatible with gene-specific regulation and suggests that it might regulate both transcriptional silencing and activation via different mechanisms (Marques et al. 2010).

H2A.Z occupancy may also influence other histone components within the nucleosome that mediate different downstream functions in transcriptional regulation. For example, H2A.Z and

[5]Corresponding author.
E-mail s.clark@garvan.org.au.
Article published online before print. Article, supplemental material, and publication date are at http://www.genome.org/cgi/doi/10.1101/gr.118919.110.

H3K27me3 are colocalized at genes with low-expression levels in embryonic stem (ES) cells, suggesting a role in potentiating gene expression (Creyghton et al. 2008). In addition, loss of H2A.Z in *Drosophila* and mammals (Greaves et al. 2007) suppresses heterochromatin formation, suggesting a role in gene suppression. H2A.Z occupancy also has been reported in plants to protect genes from DNA methylation (Zilberman et al. 2008), and this anticorrelation has now been further demonstrated in the puffer fish (Zemach et al. 2010) and in murine B-cells (Conerly et al. 2010).

Similar to other histones, H2A.Z is also subject to modification, including multiple N-terminal acetylation in *Saccharomyces cerevisiae* (Millar et al. 2006), *Tetrahymena thermophila* (Ren and Gorovsky 2001), and metazoans (Bruce et al. 2005). In yeast the H2AZ acetylation levels correlate with genome-wide gene activity (Millar et al. 2006) and is required for induction of gene transcription (Halley et al. 2010). In addition, studies in chicken erythroblast cells found that the hyperacetylated form of H2A.Z (K4, K7, and K11) (acH2A.Z) is concentrated at the 5′ end of active genes (Bruce et al. 2005) and confers nucleosome destabilization and an open conformation (Ishibashi et al. 2009).

Recently, a role for H2A.Z in gene deregulation in cancer has been suggested. The depletion of H2A.Z affects the stability and integrity of the human genome, causing the alteration of chromosome segregation (Rangasamy et al. 2004) and changes in cell cycle (Gevry et al. 2009b). A progressive depletion of H2A.Z around the transcriptional start sites (TSSs) during B-cell lymphomagenesis in the mouse has also been reported (Conerly et al. 2010). In contrast, the activation of LINE-1 transposable elements correlates with an acquisition of H2A.Z around the TSS (Wolff et al. 2010). Furthermore, *H2AFZ* gene expression is increased in several human malignancies including colorectal cancer, undifferentiated cancers, and breast cancer (Dunican et al. 2002; Rhodes et al. 2004; Zucchi et al. 2004) and also at the protein level in the case of breast cancer (Hua et al. 2008). However, the role of H2A.Z and acetylated H2A.Z in epigenetic associated deregulation of gene expression in human cancer has not been addressed.

To explore the relationship between gene expression, H2A.Z/acH2A.Z promoter occupancy, and the epigenetic repressive marks of DNA methylation and H3K27me3 in human cancer, we performed ChIP-on-chip (for histone marks) and MBDCap.seq (for DNA methylation) to characterize the epigenetic landscape in normal and prostate cancer cells. We found that while H2A.Z was associated with both active and inactive gene promoters, acH2A.Z was specific only for actively transcribed genes. Notably, in the cancer cells acetylation of H2A.Z was associated with oncogene activation and deacetylation was associated with silencing of tumor-suppressor genes (TSG). Furthermore, correlation analyses show a mutually exclusive occupancy of acH2A.Z and the repressive marks, DNA methylation and H3K27me3. The observed remodeling of promoter-associated H2A.Z and acH2A.Z with cancer-specific gene deregulation implicates a key role for the histone variant H2A.Z in tumorigenesis.

Results

H2A.Z is localized at transcription start sites of both poised and actively expressed genes

To determine the relationship between gene activity and distribution of H2A.Z within gene promoters in cancer and normal cells, we compared gene expression (Affymetrix GeneChip HuGene 1.0ST arrays) and H2A.Z ChIP-on-chip (Affymetrix Human Promoter 1.0 arrays) analyses, in normal prostate epithelial cells (PrEC), and the prostate cancer cell line LNCaP. We found that in both PrEC (Fig. 1A) and LNCaP (Supplemental Fig. 1A), the distribution of H2A.Z around TSSs differs substantially in relation to gene transcription. In inactive genes, (25% of genes, defined as expression levels RMA <4.5, see Supplementary Methods), H2A.Z was uniformly distributed across the entire promoter region (from −7500 bp to +2450 bp). In contrast, genes that were transcribed, either at poised or basal levels (expression levels 4.5–6, 25%) or medium or high levels (expression levels >6, 50%), were associated with a bimodal redistribution of H2A.Z, enriched at nucleosomes surrounding TSSs, between −1500-bp and +1000-bp regions, as previously described (Barski et al. 2007). Notably, we found that the intensity of the H2A.Z peak, located at ~500 bp upstream of TSSs, was diminished with decreasing levels of gene expression transcription. In contrast, the second H2A.Z peak, located ~500 bp downstream from TSSs, did not show significant enrichment differences in relation to gene expression. Interestingly, genes with high expression exhibit a relative loss of H2A.Z immediately after TSSs (between 0 and 250 bp). This region could correspond to a nucleosome-depleted region (NDR) (Ozsolak et al. 2007; Schones et al. 2008); however, we found that the relative depletion of histone H3 (H3) was more pronounced from +1000 to +2000 bp from TSSs in the most highly expressed genes (Supplemental Fig. 1B); a finding consistent with previous published data (Barski et al. 2007; Hardy et al. 2009; Zemach et al. 2010), suggesting that loss of nucleosomes at the TSS may not be the sole reason for the apparent bimodal promoter distribution of H2A.Z.

H2A.Z enrichment correlates with H2A depletion in actively transcribed genes

H2A.Z can assemble into either homotypic nucleosomes (consisting of H2A.Z–H2B tetramers) or heterotypic nucleosomes (consisting of one H2A.Z–H2B dimer and one H2A–H2B dimer), each having different effects on chromatin remodeling and transcription (Suto et al. 2000; Chakravarthy et al. 2004; Ishibashi et al. 2009; Weber et al. 2010). To investigate whether H2A.Z/H2A exchange is another potential epigenetic-based mechanism for gene transcriptional (de)-regulation, we determined the relative differences in H2A.Z and H2A occupancy at gene promoters according to expression levels in LNCaP and PrEC cells. Heatmap analysis of the H2A ChIP-on-chip data revealed that in both normal prostate PrEC (Fig. 1B) and cancer LNCaP cells (Supplemental Fig. 1C), there was a bimodal depletion of H2A spanning TSSs in the highly expressed genes. Notably, depleted H2A regions inversely correspond to regions showing bimodal enrichment of H2A.Z with increasing gene expression (see gene examples in Supplemental Fig. 2A). In contrast, we observed intermediate levels of both H2A and H2A.Z in the poorly transcribed and silent genes (Fig. 1A,B; see gene examples in Supplemental Fig. 2B). These results suggest that while the presence of homotypic H2A.Z nucleosomes are assembled around the TSS of actively transcribed genes, (Weber et al. 2010; Supplemental Fig. 2A,C), heterotypic nucleosomes (consisting of both H2A and H2A.Z) or a mix of both homotypic H2A-nucleosomes and H2A.Z-nucleosomes, might occur across inactive genes (Supplemental Fig. 2B,C).

Acetylation of H2A.Z is a key modification at promoters of highly expressed genes

It has previously been shown in chicken that H2A.Z can be acetylated at specific lysines (Sarcinella et al. 2007; Ishibashi et al. 2009), and both the presence of H2A.Z and its acetylation form is associated with gene activation. We therefore determined whether acetylation of H2A.Z was also correlated with active gene

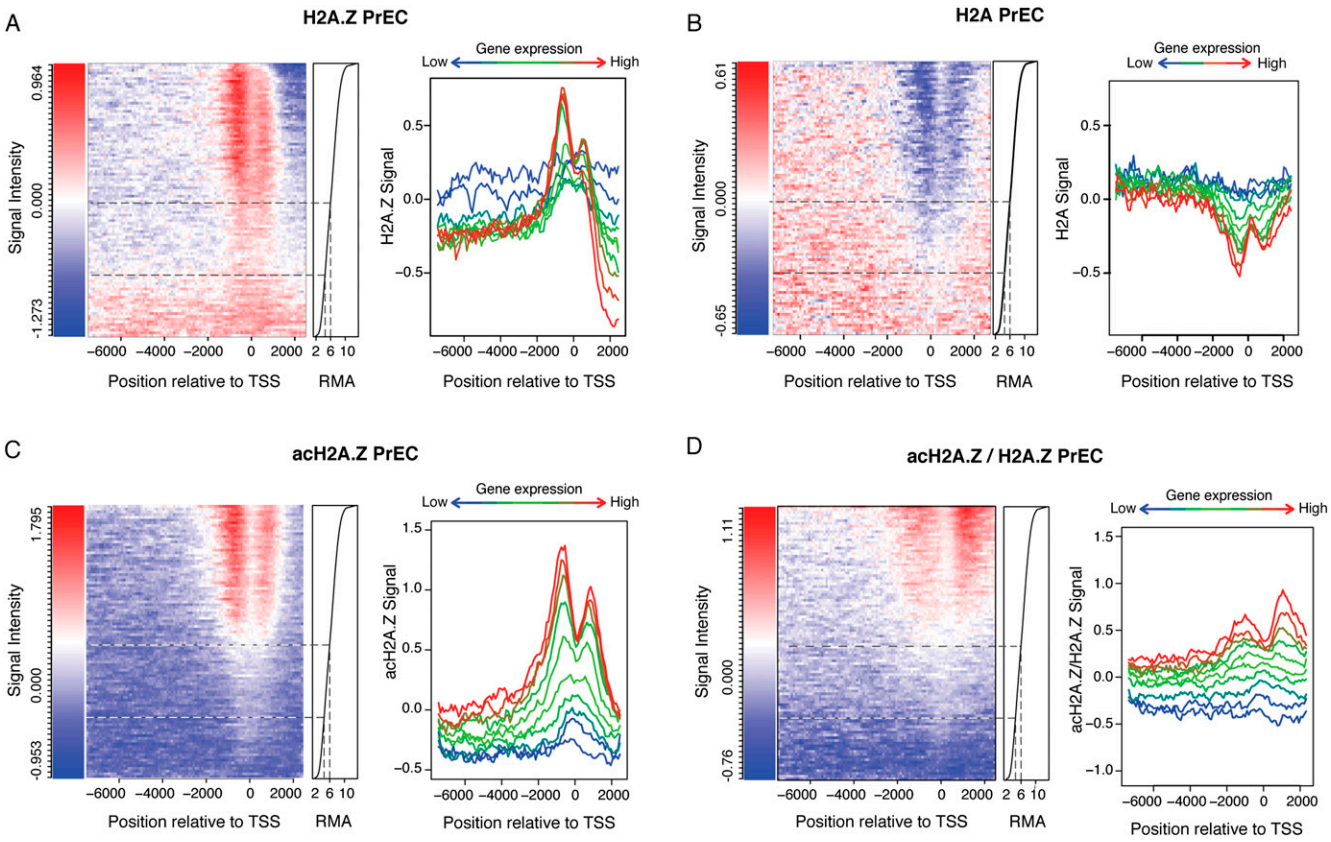

Figure 1. Correlation between gene expression and H2A.Z, H2A, acH2A.Z promoter occupancy in PrEC cells. Heatmaps (*left*) showing levels of H2A.Z (*A*), H2A (*B*), acH2A.Z (*C*), and acH2A.Z/H2A.Z (*D*) across gene promoters according to gene expression in PrEC. The *x*-axis represents promoter coordinates (−7500 bp to +2450 bp), where 0 is the transcriptional start site (TSS). Each row of the *y*-axis represents the average H2A.Z (*A*), H2A (*B*), acH2A.Z (*C*), and acH2A.Z/H2A.Z (*D*) signal intensity of 500 genes ordered according to gene expression levels (*right*), using robust multichip analysis (RMA). Antibody signal intensity (using MAT normalization) is represented from blue (low signal) to red (high signal). AcH2A.Z/H2A.Z represents acH2A.Z normalized with H2A.Z total levels. Black dotted lines demark genes either inactive (RMA < 4.5, 25% of the genes), or transcribed, either at basal levels (RMA 4.5–6, 25%) or medium or high levels (RMA > 6, 50%). Line plots (*right*) for H2A.Z (*A*), H2A (*B*), acH2A.Z (*C*), and acH2A.Z/H2A.Z (*D*) show enrichment in PrEC according to different levels of expression. Gene expression levels were split in groups of 2500 genes (blue for low expressed genes; green to red for high expressed genes). The average signal of the specific group was plotted along the gene promoter.

expression in the prostate normal and cancer cells. Using an antibody specific for acH2A.Z (Bruce et al. 2005), we found that acetylation of H2A.Z was restricted to the proximal promoters of only the active genes (expression levels >6, 50% of the genes) in both normal (Fig. 1C) and cancer cell lines (Supplemental Fig. 1D). For H2A.Z, there was a bimodal distribution observed around the TSS, but with more pronounced enrichment with increasing with gene expression levels (expression levels >6); which was further augmented when acH2A.Z was normalized to the levels of total H2A.Z (comprising both the acetylated and underacetylated forms; see Supplemental Methods; Fig. 1D; Supplemental Fig. 1E). However, unlike H2A.Z distribution, there was a clear lack of acH2A.Z in both the poised/lowly expressed genes (expression levels 4.5–6, 25% of the genes) and inactive genes (expression levels <4.5, 25%) (Fig. 1C,D; Supplemental Fig. 1C,D). Notably, the acH2A.Z profiles, relative to gene expression, were similar to the profiles of the active chromatin marks H3K9 acetylation (H3K9ac) and H3K4 trimethylation (H3K4Me3) (Bernstein et al. 2005); with a similar bimodal distribution across the TSSs of active genes, but dissimilar to the repressive H3K27 trimethylation (H3K27me3) chromatin mark that is depleted across the entire gene promoter of active genes (Supplemental Fig. 3).

Acetylation of H2A.Z is correlated with gene deregulation in prostate cancer

We next investigated the role of H2A.Z and its post-translational modification in deregulation of gene expression in prostate cancer. First, we compared the changes of H2A.Z occupancy along the promoter of genes that were deregulated in LNCaP cancer cells relative to PrEC (Fig. 2A). In LNCaP cells, we observed a significant relocalization of H2A.Z downstream from the TSS, including part of gene bodies (from +1000 bp to +2450 bp), with a gain of H2A.Z in the most repressed genes and loss of H2A.Z in the most activated genes. However around TSSs, we observed a minor depletion of H2A.Z, primarily in actively transcribed genes (Fig. 2A). We also observed a moderate increase in H2A occupancy from −4000 bp in the down-regulated genes (Fig. 2B), but no other H2A or H2A.Z changes were found across promoters of deregulated genes. Next, we investigated whether acH2A.Z was associated with transcriptional deregulation in LNCaP cells and analyzed levels of absolute acH2A.Z (Fig. 2C) and relative acH2A.Z (acH2A.Z/H2A.Z) along the entire promoter regions (Fig. 2D). We found that the most down-regulated genes (blue line) exhibited a loss of both acH2A.Z and acH2A.Z/H2A.Z along the entire

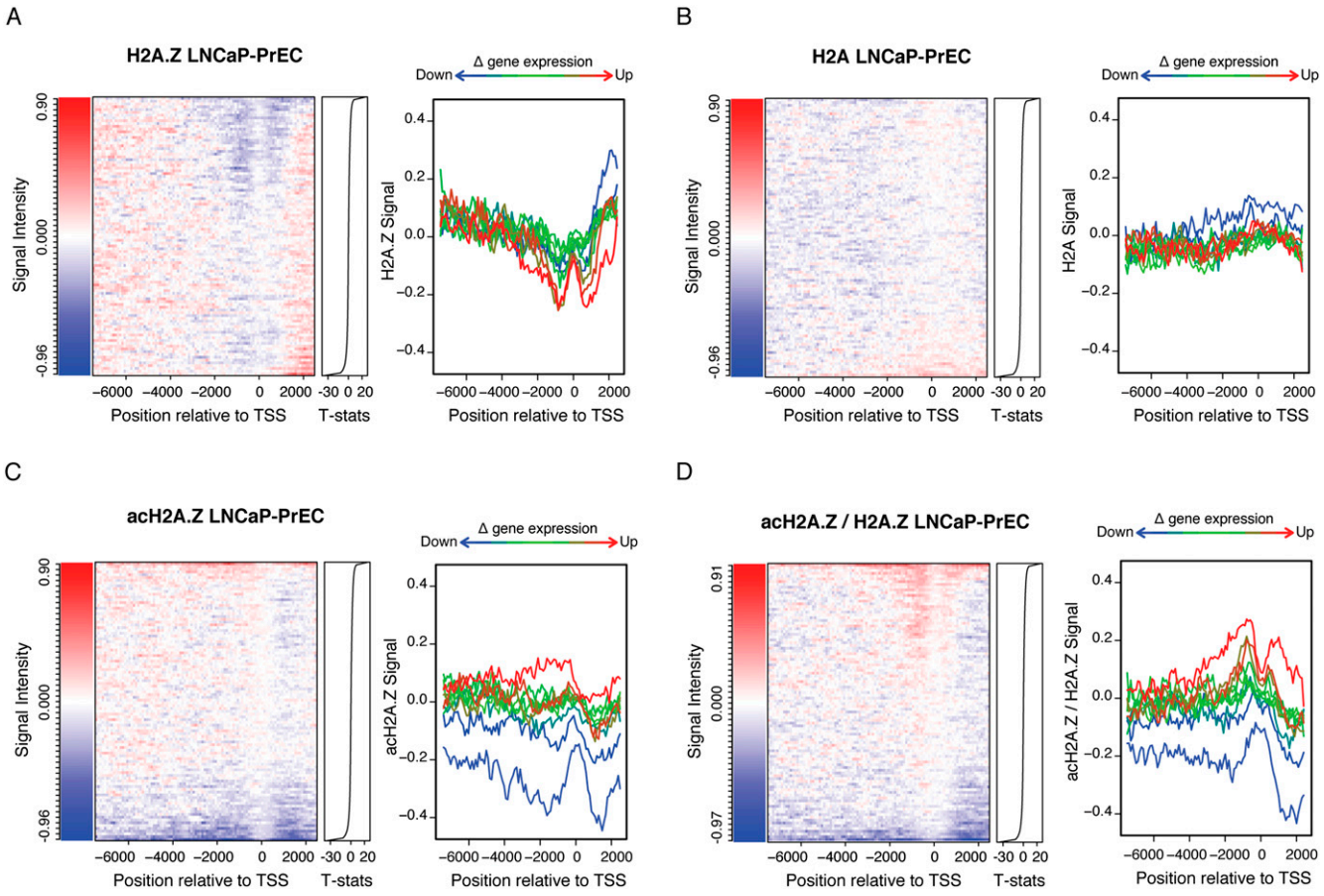

Figure 2. H2A.Z, H2A, and acH2A.Z occupancy changes with gene deregulation in prostate cancer. Heatmaps (*left*) and line plots (*right*) for H2A.Z (*A*), H2A (*B*), acH2A.Z (*C*), and acH2A.Z/H2A.Z (*D*) were made according to changes in gene expression in LNCaP relative to PrEC (LNCaP-PrEC), represented as a moderated t-statistics (T-stats), to study nucleosome occupancy with changes in gene expression. For heatmaps, genes were sorted into groups of 500 genes, according to changes in gene expression in LNCaP-PrEC, from down-regulated (*bottom*) to up-regulated (*top*). The color scale represents changes in signal intensity of each antibody (using a two-sided *t*-test), between LNCaP and PrEC from blue (loss of signal) to red (gain of signal). For line plots, groups of 2500 genes were generated according to changes in gene expression in LNCaP-PrEC. The *y*-axis represents the average change in each antibody between LNCaP and PrEC. Line colors are as described for Figure 1.

promoter, indicating that either deacetylation or lack of reacetylation occurs with gene inactivation. Conversely, in the most up-regulated cancer genes (red line), levels of absolute acH2A.Z exhibited a gain from −3000 bp to the TSS, whereas the level of relative acH2A.Z exhibited a stronger signal with two discrete peaks of gain around TSSs.

Exchange between H2A.Z and acH2A.Z-containing nucleosomes in prostate cancer

We have demonstrated that acH2A.Z levels are tightly associated with an increase in transcriptional activity and vice versa in prostate cancer. Conversely, H2A.Z is reorganized at gene promoters according to transcriptional levels; however, this mechanism appears independent of gene deregulation. Given that, unlike H3, H2A.Z is not constant among gene promoters, we wanted to further analyze whether differential levels of acH2A.Z/H2A.Z could result from differential distribution of acH2A.Z and H2A.Z. A gene list was created of the most up-regulated genes (25% of the genes) (Fig. 3A, red line) and down-regulated genes (25% of the genes) (Fig. 3A, blue line) in LNCaP cells. Of the 2153 overexpressed genes, 1552 (72%) had increased acH2A.Z/H2A.Z levels in LNCaP (levels of acH2A.Z/H2A.Z presence using two-sided *t*-test, t-stats > 0). Of the 2110 down-regulated genes, 1391 (65%) genes had a loss of acH2A.Z/H2A.Z (t-stats > 0). We then selected from the overexpressed list, the genes with the highest levels of acH2A.Z/H2A.Z (545 genes, acH2A.Z/H2A.Z t-stats ≥ 1.5; Supplemental Table 1) and those that had the greatest loss of acH2A.Z/H2A.Z (479 genes t-stats ≤ −1.5; Supplemental Table 2). We found that the 479 down-regulated cancer genes showing a loss of acH2A.Z/H2A.Z (Fig. 3B, blue boxes, "Down"), exhibited a significant gain of H2A.Z and concurrent loss of acH2A.Z across the promoter (−2000 bp to +1500) region, suggesting that H2A.Z deacetylation is predominately associated with gene repression in prostate cancer cells. Figure 3C shows screen shots of representative gene promoter examples including *NFKB1, SERPINB5*, and *ANXA1*. These findings indicate that gene repression in cancer is not a result of a total loss of H2A.Z, but a loss of acH2AZ. This suggests that genes that exist in a poised state could potentially be reactivated by acetylation of H2A.Z. Conversely, in the up-regulated genes that show a gain of acH2A.Z/H2A.Z (Fig. 3B, red boxes, "Up") we found a significant loss of H2A.Z and a gain of acH2A.Z, suggesting that promoter-associated H2A.Z is predominately acetylated in activated

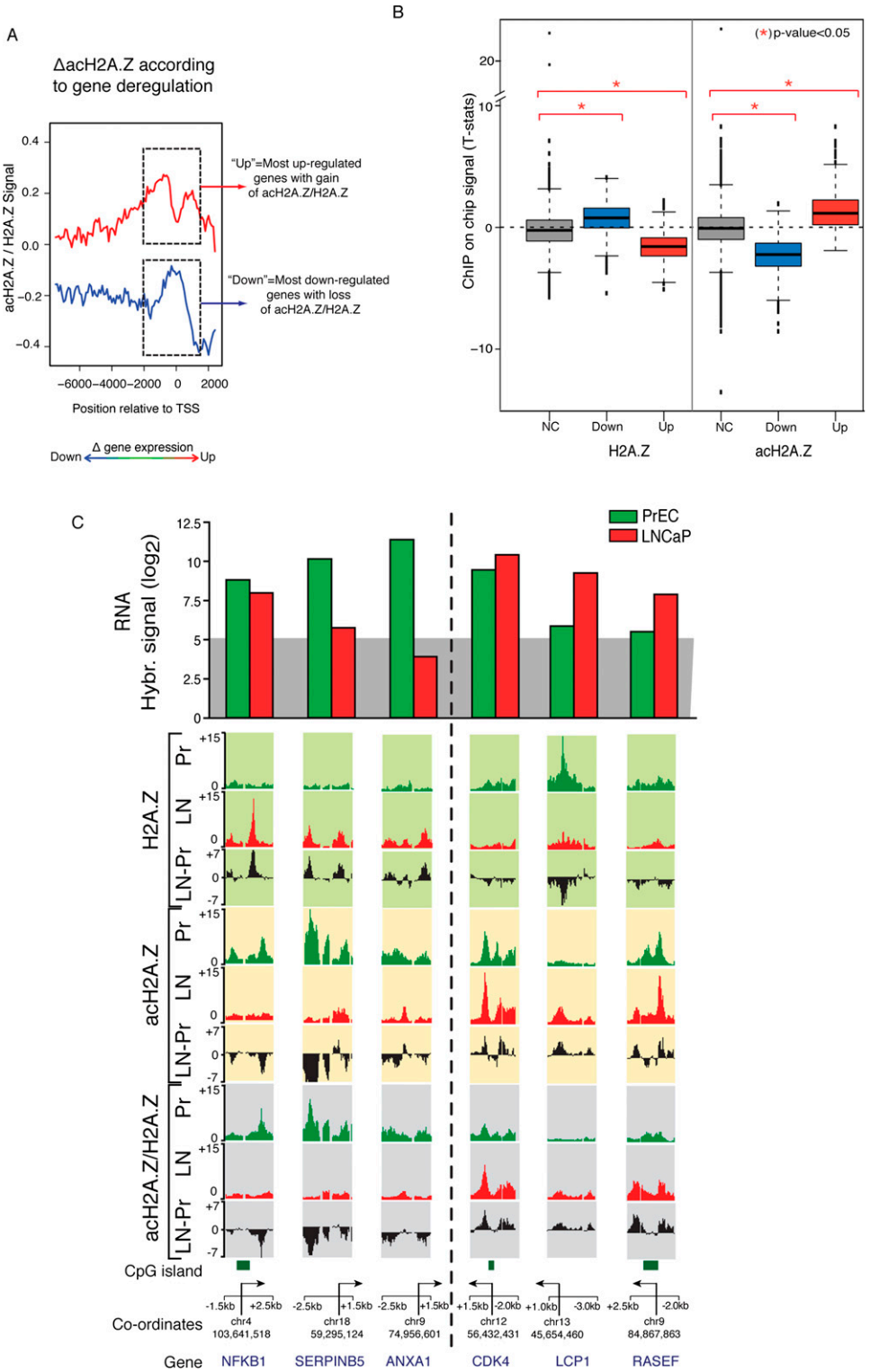

Figure 3. Opposing changes in H2A.Z and acH2A.Z occupancy is a potential mechanism of transcriptional (de)regulation. (*A*) Line plots of acH2A.Z/H2A.Z changes in LNCaP compared to PrEC. Top 25% up-regulated genes (red line) and top 25% down-regulated genes (blue line), across the promoter region, −2000 bp to +1500 bp highlighted in hatched boxes. "Up": top up-regulated genes show a gain of acH2A.Z /H2A.Z. "Down": top down-regulated genes show a loss of acH2A.Z/H2A.Z. (*B*) Box plots display the significance of change between H2A.Z and acH2A.Z levels. *y*-axis: distributions of t-statistics (H2A.Z and acH2A.Z) with change in expression. *x*-axis: "NC" (no change in expression, gray boxes); "Down" (down-regulated genes, blue boxes); "Up" (up-regulated genes, red boxes). The *P*-values of significance of differences between box plots were obtained with the *limma* function geneSetTest where (*) means a *P*-value of <0.05. (*C*) (*Top*) Microarray hybridization signals for mRNA expression levels in LNCaP (red) and PrEC (green) of three representative oncogenes from Table 1 (*left*), and three tumor suppressor genes (TSG) from Table 2 (*right*). Gray background highlights signals below detection (<5.0). UCSC Genome Browser tracks (*bottom*) for H2A.Z (green background), acH2A.Z (yellow background), and acH2A.Z/H2A.Z (gray background). Enrichment over input status and differential pattern shown. Pr (green tracks): PrEC; LN (red tracks): LNCaP; LN-Pr (black tracks): LNCaP minus PrEC. TSS for each gene shown as an arrow, genomic coordinates are indicated and CpG islands are depicted by green boxes. The scale of UCSC tracks is represented as the distance in kilobases (kb) upstream of "−" and downstream from "+" the TSS.

prostate cancer genes. Figure 3C shows screen shots of representative gene examples including *CDK4, LCP1*, and *RASEF*.

Prostate cancer oncogenes and tumor-suppressor genes have altered acH2A.Z /H2A.Z promoter occupancy

We next identified known key genes involved in carcinogenesis that exhibited altered expression in LNCaP cells to determine whether the change in acH2A.Z/H2A.Z promoter levels are associated with their transcriptional alteration. Table 1 summarizes a subset of genes from Supplemental Table 1 that are reported oncogenes in prostate cancer, including *KLK2, C15orf21*, and *ERBB3* (Futreal et al. 2004) (http://www.sanger.ac.uk/genetics/CGP/Census/). Table 2 summarizes a subset of genes from Supplemental Table 2 that are reported TSG in prostate cancer, including *CAV1, CAV2*, and *RND3* (Higgins et al. 2007) (http://cbio.mskcc.org/CancerGenes/Select.action). We validated the change in expression and H2A.Z and acH2A.Z promoter level occupancy of three up-regulated oncogenes (*KLK2, C15orf21*, and *ERBB3*) and three down-regulated TSG (*CAV1, CAV2*, and *RND3*) in LNCaP and PrEC cells from the gene expression and ChIP-on-chip data (Fig. 4A). We confirmed in prostate cancer cells by qRT–PCR (Fig. 4B), that gene activation or repression was inversely correlated with acetylation or deacetylation of H2A.Z, respectively, with the exception of the *ERBB3* gene. Furthermore, treatment of LNCaP cells with the deacetylase inhibitor Trichostatin A (TSA) results in concordant gene activation and gain of the acH2A.Z mark across the TSS of repressed genes, (for example, *CAV1* and *CAV2*) (Fig. 5A). In addition, active genes (for example *LIMCH1, KLK2*, and *KLK3*) can be further activated after TSA treatment, in association with an increase in acetylation of H2A.Z (Fig. 5B). Conversely, LNCaP cells treated with Anarcardic Acid (AA), an inhibitor of histone acetyl transferases (HATs) (Balasubramanyam et al. 2003) resulted in deacetylation of H2A.Z and consequent transcriptional repression of genes that harbor high levels of acH2AZ at gene promoters such as *KLK2*, *C15orf21*, and *KLK3* (Fig. 5C). This data combined supports a potential mechanistic link between the acetylation status of H2A.Z and active gene transcription. We have also validated the direct association between changes in acH2A.Z and changes in gene expression in two additional prostate cancer cell lines PC-3 and DU-145, demonstrating that the association is not cell line dependent (Fig. 5D).

H2A.Z and acH2A.Z nucleosome occupancy is anticorrelated with DNA methylation in cancer cells

Next we determined whether there was an inverse relationship between H2A.Z and acH2A.Z occupancy and DNA methylation in prostate cancer cells, as H2A.Z occupancy has been reported (Zilberman et al. 2008; Conerly et al. 2010; Zemach et al. 2010) to be antagonistic to DNA methylation. We compared the DNA methylation profile of PrEC and LNCaP cells, using MBDCap.seq, with H2A.Z and acH2A.Z ChIP-on-chip data (Fig. 6A). We found a significant correlation between highly methylated genes (red line) and low H2A.Z and acH2A.Z occupancy around the TSS in both normal and cancer cells. Conversely, genes that are lowly or completely unmethylated (black line) have a significant increase in H2A.Z and acH2A.Z levels. Interestingly, the opposite pattern was observed for H2A deposition, where H2A nucleosomes positively correlated with high levels of DNA methylation, whereas genes poorly methylated were depleted in H2A associated nucleosomes (Supplemental Fig. 4).

We next asked whether genes that became either hyper- or hypomethylated in LNCaP cells, compared with PrEC cells, also underwent a concordant change in the H2A.Z modification. Genes were plotted according to promoter hypermethylation in the cancer cell (≥2-fold more methylated in LNCaP than PrEC, 3150 genes; see Supplemental Methods) or hypomethylation (≥2-fold less methylated in LNCaP than PrEC, 225 genes). A trend was observed for gain of acH2A.Z in hypomethylated genes, but no significant anticorrelation between DNA methylation and H2A.Z nor acH2A.Z occupancy was found (Supplemental Fig. 5). To test the hypothesis that an anticorrelation only occurred in gene promoters that changed in cancer-associated gene expression, we sorted the gene lists according to changes in DNA methylation and gene expression. We found that 903 hypermethylated genes exhibited significant gene silencing (expression t-stats ≤ -1.5) and 75 hypomethylated genes were activated (expression t-stats ≥ 1.5) in the cancer cells (Supplemental Tables 3, 4). Using this criteria, a significant anti-

Table 1. Oncogenes associated with a loss of acH2A.Z/H2A.Z

Gene symbol	T-stats expression	T-stats diff H2A.Z (−2000 to +1500 bp)	T-stats diff acH2A.Z (−2000 to +1500 bp)	T-stats diff acH2A.Z/H2A.Z (−2000 to +1500 bp)	Fold change MBDCap (−2000 to +1500 bp)	T-stats diff K27me3 (−1000 to +1000 bp)	Oncogene in prostate cancer (PC)
KLK2	16.67	−0.62	6.81	5.74	−1.36	−5.36	PC
CDK4	3.20	−2.60	1.43	3.09	−2.99	0.18	
IDH1	5.66	−3.68	−0.47	2.70	3.33	0.19	
HLF	9.68	−1.05	2.75	2.53	2.97	−3.41	
C15orf21	5.64	0.39	4.55	2.44	−0.33	−4.15	PC
LCP1	4.42	−1.93	1.35	2.23	−0.41	−2.58	
BCL6	7.68	−2.99	−0.75	2.14	0.30	−0.66	
IDH2	7.07	−2.84	−0.50	2.13	2.79	1.05	
PRCC	3.37	−0.48	3.48	2.01	−0.55	0.59	
GPC3	8.20	−1.29	1.10	1.65	1.02	−2.33	
NCOA2	3.87	−2.51	−0.34	1.58	3.29	1.06	
RASEF	10.10	−2.15	1.43	2.81	−0.85	−2.04	
CASC4	4.77	−2.77	0.28	2.71	0.78	−0.33	
ERBB3	7.33	−0.96	2.38	2.61	0.00	−0.07	PC
AFF3	14.69	1.00	4.85	2.28	1.64	−5.48	
RAB3B	5.17	−0.94	1.05	1.64	−1.59	−1.92	
FRAT1	3.24	−0.53	2.12	1.60	1.91	1.62	

Sanger and Cbio MSKCC resources. Shaded rows: Oncogene reported in prostate cancer.

Table 2. Tumor suppressor genes associated with a loss of acH2A.Z/H2A.Z

Gene symbol	T-stats expression	T-stats diff H2A.Z (−2000 to +1500 bp)	T-stats diff acH2A.Z (−2000 to +1500 bp)	T-stats diff acH2A.Z/H2A.Z (−2000 to +1500 bp)	Fold change MBDCap (−2000 to +1500 bp)	T-stats diff K27me3 (−1000 to +1000 bp)	TSG in prostate cancer (PC)
INHBA	−9.59	2.00	−3.57	−4.13	4.78	1.97	
CAV1	−23.80	0.41	−4.35	−3.73	1.68	4.77	PC
CLCA2	−13.24	−1.83	−9.27	−3.55	−0.72	1.55	
SFN	−21.09	2.83	−1.87	−3.36	9.43	−1.03	PC
IL1B	−16.39	0.32	−4.32	−3.28	0.41	0.82	
TP63	−18.58	0.89	−3.33	−3.08	2.94	−1.30	PC
CAV2	−28.24	1.17	−3.22	−3.05	5.67	1.75	PC
CDKN1A	−3.51	3.19	−0.57	−2.95	0.88	−1.13	PC
AIFM2	−3.63	−0.10	−4.10	−2.81	3.95	0.98	
NFKB1	−3.21	1.78	−1.97	−2.72	−0.39	1.51	PC
JUP	−4.90	1.73	−1.43	−2.42	0.00	2.29	
LIF	−3.62	1.00	−2.53	−2.34	1.25	1.74	
CCND2	−29.74	0.80	−2.03	−2.20	7.82	1.72	PC
SERPINB5	−15.92	1.43	−1.55	−2.19	−0.11	0.93	PC
SPRY2	−8.61	0.60	−3.08	−2.18	6.63	2.29	PC
GJB2	−8.08	1.28	−1.63	−2.12	−0.64	0.36	
RBBP8	−7.05	3.01	0.34	−2.03	−2.12	−0.04	
SMAD3	−8.00	0.74	−2.27	−2.03	3.59	1.02	PC
DKK1	−11.38	0.02	−2.85	−1.89	5.81	2.48	PC
DAB2IP	−3.23	2.31	−0.18	−1.85	−0.32	1.47	PC
ANXA1	−31.55	0.96	−1.69	−1.84	−0.73	0.03	PC
PML	−3.00	2.49	0.27	−1.81	0.91	−0.25	PC
PHLDA2	−3.32	1.43	−0.71	−1.72	1.98	1.05	
DKK3	−10.43	1.42	−0.83	−1.66	2.28	2.93	PC
NFKB2	−3.52	1.96	−0.33	−1.64	0.09	2.21	
RND3	−11.92	0.43	−1.84	−1.58	3.10	2.19	PC
MET	−26.96	0.47	−1.61	−1.52	6.06	0.82	PC

Cbio MSKCC resource. Boldface: Prostate TSG contained in 903 hypermethylated gene list. Shaded rows: TSG reported in prostate cancer.

correlation was observed only for acH2A.Z, but not for H2A.Z (Fig. 6B). We validated the inverse relationship between acH2A.Z and DNA methylation and expression using qRT–PCR, acH2A.Z, and H2A.Z ChIP qPCR and Sequenom methylation analysis (Coolen et al. 2007) on three genes (*MKRN3, LIMCH1* and *RND3*) from Table 2 and Supplemental Table 4 that showed changes in methylation (Fig. 6C; Supplemental Fig. 6). In addition, we previously described changes in DNA methylation of *CAV1* and *CAV2* genes between LNCaP and PrEC cells (Coolen et al. 2010), which also confirmed this mutual exclusion. Together, this data supports the conclusion that it is the acetylation of H2A.Z that is anticorrelated with DNA methylation and gene activity and not H2A.Z itself. Our results suggest an epigenetic mechanistic link where deregulated genes in prostate cancer present opposite changes between DNA methylation and the acetylation state of H2A.Z.

H2A.Z and acH2A.Z promoter presence is anticorrelated with H3K27me3

H2A.Z and H3K27me3 are enriched at genes with low-expression levels in ES cells, although this pattern is not maintained in multipotent neural precursors (Creyghton et al. 2008). In order to study the relationship between H2A.Z and the polycomb mark, we compared H2A.Z and acH2A.Z with H3K27me3 ChIP-on-chip data. H2A.Z and acH2A.Z status was filtered in two groups: H2AZ or acH2A.Z high (t-stats > 1.5) and low (t-stats < −1.5), where the K27Me3 ChIP-on-chip average signal was plotted along promoter region in PrEC and LNCaP (Fig. 7A). Consistent with previous data demonstrating H2A.Z and acH2A.Z as an active chromatin mark surrounding the TSS, we observed a significant anticorrelation between K27Me3 and H2A.Z, acH2A.Z, and acH2A.Z/H2A.Z (Fig. 7A). The same criteria were established to study whether this anticorrelation occurs in the cancer cells, which could suggest a relevant role in gene deregulation during prostate cancer development and progression. Figure 7B shows a significant anticorrelation between the polycomb mark H3K27Me3 and acH2A.Z and acH2A.Z/H2A.Z, but not for H2A.Z. We confirm this anticorrelation in prostate cancer for *CAV1, RND3, KLK2* and *LIMCH1* by qPCR (Fig. 7C). In LNCaP cells, *CAV1* and *RND3* genes were enriched in H3K27Me3 (Fig. 7C) in the same region that acH2A.Z/H2A.Z is lost (Fig. 4B). In addition, *KLK2* and *LIMCH1* genes showed decreased H3K27Me3 levels (Fig. 7C), whereas acH2A.Z/H2A.Z is increased in LNCaP cells (Figs. 4B, 7C). We conclude that the anticorrelation between acH2A.Z and H3K27Me3 might also play a critical role in the deregulation of gene expression in prostate cancer.

Discussion

A new epigenetic H2A.Z acetylation model for the regulation of transcription

The role of the histone variant H2A.Z in epigenetically regulated gene expression remains controversial with conflicting reports of its role in both active and inactive gene expression in different model systems. In this study, we characterized the nucleosome occupancy of H2A.Z and acetylation status in human gene promoters to determine its role in epigenetic remodeling and gene deregulation in prostate cancer cells. We found that the landscape of H2A.Z promoter occupancy and its acetylation state directly correlates with the level of gene expression, arguing that acetylation of H2A.Z plays a key role in gene regulation in normal cells and gene deregulation in cancer. Figure 8 summarizes our data in a model where we find

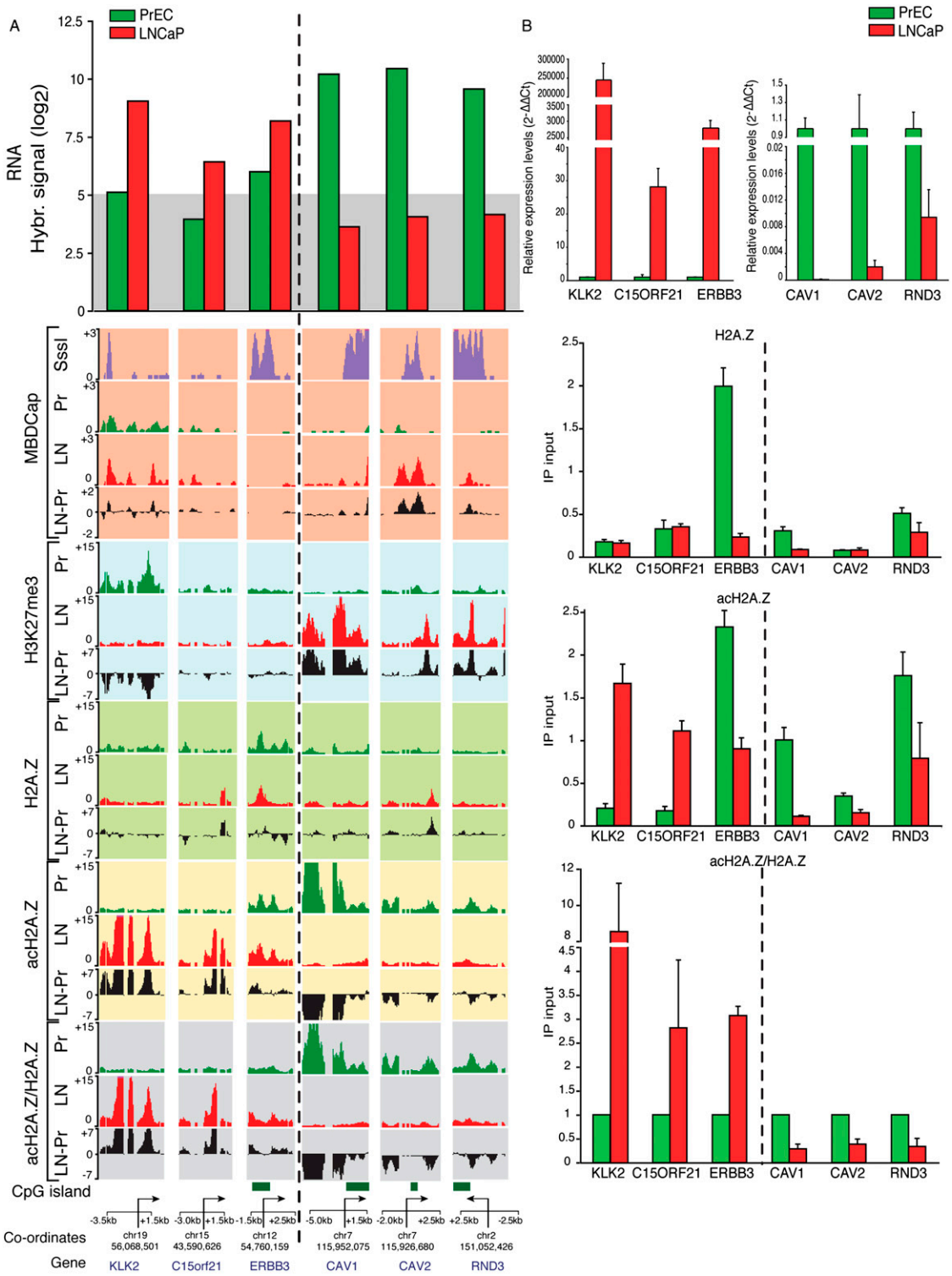

Figure 4. Prostate cancer–related gene deregulation shows opposite acH2A.Z/H2A.Z promoter enrichment profiles. (*A*) Microarray hybridization signals for mRNA expression levels in LNCaP (red) and PrEC (green) of three example oncogenes: *KLK2*; *C15orf21;* and *ERBB3;* and three example TSGs: *CAV1, CAV2*, and *RND3* (*top*). (*Bottom*) UCSC Genome Browser tracks for DNA methylation (MBDCap.seq, red background), H3K27me3 (blue background), H2A.Z, acH2A.Z and acH2A.Z/H2A.Z ChIP-on-chip profiles. SssI (violet tracks): fully methylated positive control DNA. (*B*) Validation of tiling array, gene expression, and ChIP-on-chip data for H2A.Z, acH2A.Z, and acH2A.Z/H2A.Z using real-time qPCR. Relative mRNA levels normalized using *GAPDH*. For ChIP data, all samples were normalized with their corresponding Input chromatin and represented as $2^{-\Delta CT}$ (see Methods). H2A.Z and acHA.Z data are representative examples of three independent experiments; acH2A.Z/H2A.Z is represented as fold change of LNCaP relative to PrEC (mean of the fold change ±SEM). Note, for the *ERBB3* gene, there is a gain of the relative acetylation of H2A.Z (acH2A.Z/H2A.Z fold enrichment) in LNCaP cells due to the relative depletion of total H2A.Z in this region (H2A.Z IP). Abbreviations, colors, and symbols are the same as in Figure 3.

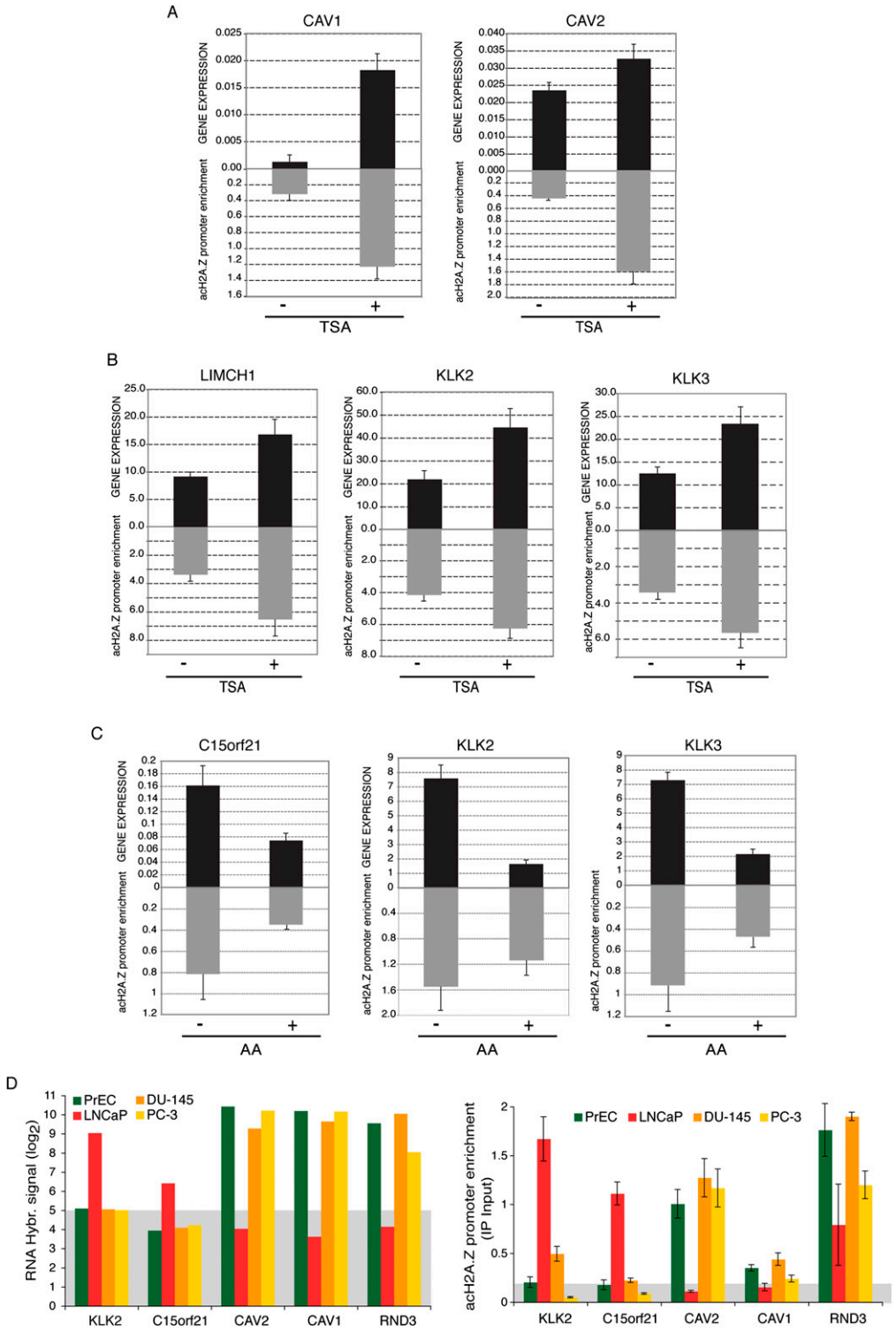

Figure 5. Acetylation of H2A.Z correlates with gene activation in prostate cancer. (*A*) LNCaP cells were either untreated (−) or treated (+) with Trichostatin A (TSA) at 100 nM for 48 h. Gene expression levels of *CAV1* and *CAV2* (*A*) or *LIMCH1*, *KLK2*, and *KLK3* (*B*) genes were measured by RT–qPCR, and acH2A.Z levels at TSSs were measured by ChIP qPCR. Relative mRNA levels were normalized using *ALAS1*. A concordant increase in acH2A.Z and gene activation, after TSA treatment was observed for all genes. (*C*) LNCaP cells were either untreated (−) or treated (+) with Anacardic Acid (AA) at 90 μM for 48 h. Gene expression levels of *C15orf21*, *KLK2*, and *KLK3* genes were measured by RT–qPCR, and acH2A.Z levels at the TSS were measured by ChIP qPCR. Relative mRNA levels were normalized using *ALAS1*. A concordant decrease in acH2A.Z and gene repression, after AA treatment, was observed. (*D*) (*Left*) Microarray hybridization signals for mRNA expression levels in PrEC (green), LNCaP (red), DU-145 (orange), and PC-3 (yellow) of five gene examples *KLK2*, *C15orf21*, *CAV2*, *CAV1*, and *RND3*. (*Right*) acH2A.Z ChIP qPCR at the promoter region of *KLK2*, *C15orf21*, *CAV2*, *CAV1*, and *RND3* as per Figure 4. Gray background in the *bottom* panel highlights an arbitrary threshold for the minimum acH2A.Z signal associated with gene activation. Acetylation of H2A.Z correlates with gene activation in all gene examples.

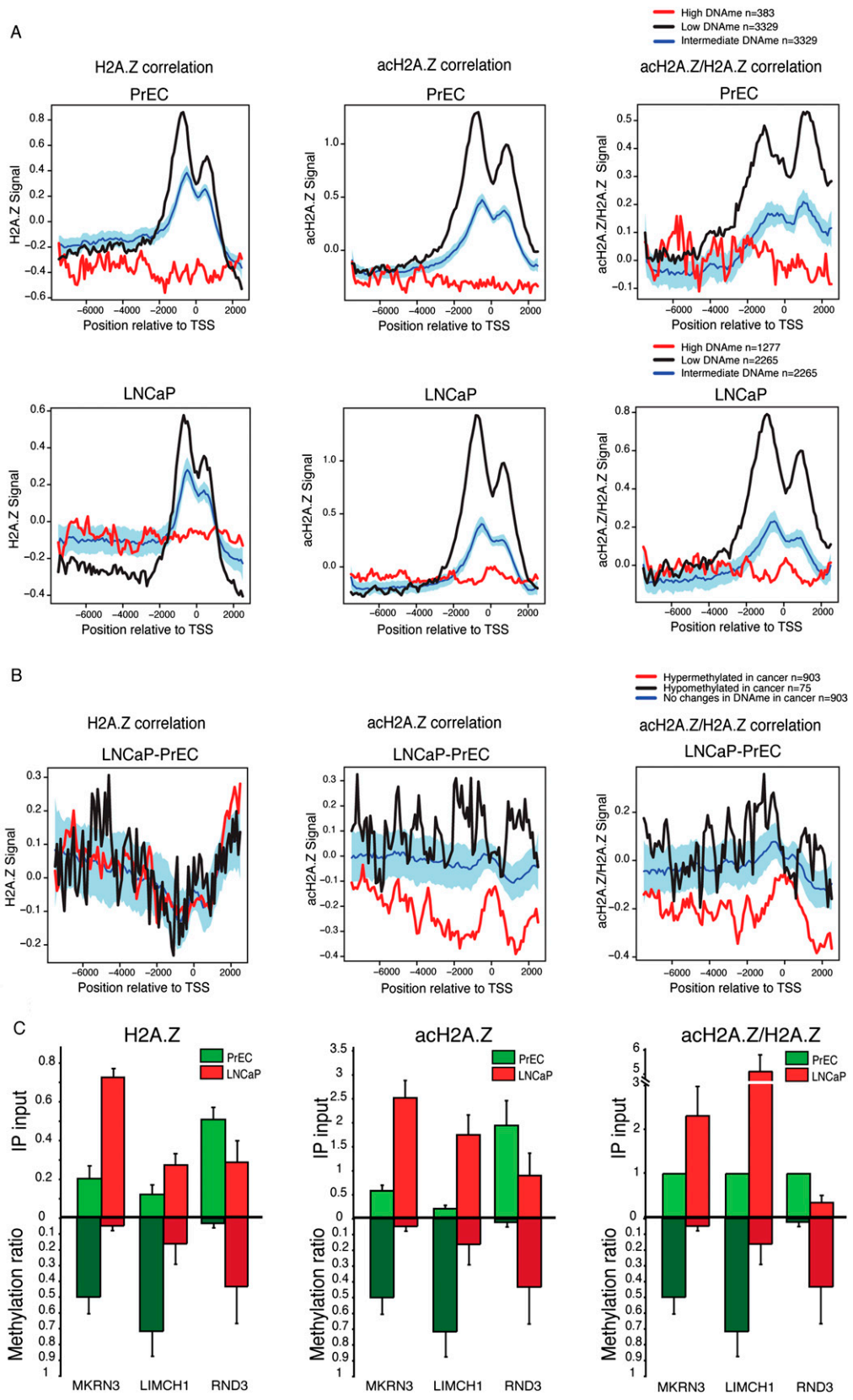

Figure 6. (Legend on next page)

a bimodal pattern of H2A.Z occupancy across the TSSs of both basal/poised and expressed genes, whereas uniform distribution of H2A.Z occurs across the gene promoters of inactive genes. We show for the first time that it is acetylation of H2A.Z-occupied nucleosomes at TSSs that potentially drives active gene expression in normal cells, and deacetylation of H2AZ that drives gene repression in cancer cells, rather than a change in H2A.Z occupancy alone.

Acetylation of H2A.Z around the TSS is a mark of active genes

Our results support previous findings that show high enrichment of H2A.Z at promoter regions (Barski et al. 2007), spanning at least −3 to +3 nucleosomes of actively transcribed genes in the human genome (Schones et al. 2008). However, our data also suggest that the region upstream of the TSS, which is more enriched in H2A.Z, might contribute to gene activity by maintaining chromatin accessibility for transcription-factor binding and RNA poll II recruitment (Hardy et al. 2009). Indeed, the enrichment of H2AZ nucleosomes at promoters has been shown to increase the nucleosome turnover rate in yeast (Dion et al. 2007), suggesting a more mobile nature of H2A.Z-containing nucleosomes. It has also been proposed that H2A.Z is associated with chromatin that has architecture suitable for either activation or repression of local genes (Guillemette and Gaudreau 2006). We show that the transcriptional state appears to be determined by a specific post-translational modification to H2A.Z. It has previously been shown that mammalian H2A.Z can be acetylated or monoubiquitylated at specific lysines (Sarcinella et al. 2007; Ishibashi et al. 2009). Our results demonstrate that H2A.Z is only hyperacetylated surrounding the TSSs of actively transcribed genes and not in genes poised or lowly transcribed. In addition, we observe a gain of H2A.Z acetylation at TSSs after histone deacetylation (HDAC) drug-induced gene activation, and conversely, a loss of acH2A.Z after histone acetyltransferase (HAT) drug-induced gene repression, suggesting a functional link between these two events. Acetylation of H2A.Z is also reported to be associated with active gene promoters in other organisms, and this modification is thought to be important for the conformational change of nucleosomes (Ishibashi et al. 2009).

Silent genes harbor both H2A and H2A.Z across the entire promoter

Interestingly, some studies have reported H2A.Z to be absent from inactive genes (Bruce et al. 2005), and other studies have found H2A.Z to be involved in negative regulation of transcription reporting high levels at heterochromatic regions (Hardy et al. 2009). We find in human cells that inactive genes, in contrast to active or lowly transcribed genes, contain both H2A and H2A.Z distributed evenly across the whole promoter. It is unclear whether H2A.Z and H2A occur as homotypic nucleosomes randomly distributed across repressed promoters, or whether both histones are contained in the same nucleosome to constitute heterotypic nucleosomes (Chakravarthy et al. 2004; Viens et al. 2006; Ishibashi et al. 2009). A previous study showed that heterotypic coexistence of H2A and H2A.Z in a nucleosome did not have significant effects on its stability or its conformation, but the coexistence of acetylation marks could mediate destabilization of chromatin (Ishibashi et al. 2009). Therefore, a combination of histone post-translational modifications within heterotypic nucleosomes would potentially affect its stability, leading to alterations in gene transcription. However, Weber et al. (2010) reported that structural differences between heterotypic and homotypic nucleosomes contributed to the localization and function of H2AZ in *Drosophilia*. Our results suggest that this may also be conserved in mammals, where H2A–H2A.Z replacement only takes place in actively transcribed genes, while hybrid nucleosomes are the predominant form in lowly expressed genes, generating another level of structural and functional heterogeneity in chromatin. ChIP–reChIP assays experiments, however, are needed to further demonstrate the presence of heterotypic nucleosomes.

Deregulation of gene expression in cancer accompanies remodeling of the acH2A.Z/H2A.Z promoter landscape

We show for the first time that there is an alteration in the acetylation pattern of H2A.Z across the TSS of genes in prostate cancer cells, and this is strongly associated with changes in gene expression. Down-regulated genes exhibit a gain of hypoacetylated H2A.Z at proximal promoters (Fig. 8A). However, it is still unresolved whether H2A.Z is deacetylated by HDACs or whether there is histone exchange (Lu et al. 2009). It is interesting to note that down-regulated genes still contain H2A.Z at their promoters, suggesting that rather than being permanently silenced, these genes are potentially capable of reactivation. Conversely, activated genes in the cancer cells gain hyperacetylated H2A.Z (Fig. 8B), but again, it is unclear whether this is a result of active acetylation by a histone acetyltransferase (HAT) prior to, or during transcription (Millar et al. 2006), or due to nucleosome exchange with acetylated H2A.Z (Doyon and Cote 2004; Mizuguchi et al. 2004).

In particular, we have found that H2A.Z reorganization was common and occurred in a significant number of genes involved in development and progression of prostate cancer (Tables 1, 2). Interestingly, overexpression of H2A.Z promotes cell proliferation in breast cancer (Gevry et al. 2009a,b), and increased gene expression of *H2AFZ* has been reported in several major types of malignancies (Dunican et al. 2002), suggesting that in the light of our new data this may be due to an increase in the available H2AZ for acetylation. In contrast, a progressive depletion of H2A.Z around TSSs during murine lymphomagenesis has been described correlating with a loss of gene expression (Rhodes et al. 2004; Zucchi et al. 2004; Hua et al. 2008; Conerly et al. 2010). Our work suggests a new mechanism for gene deregulation in cancer through changes in H2A.Z occupancy

Figure 6. Anticorrelation between DNA methylation and H2A.Z or acH2A.Z in human prostate cancer. (*A*) Significance plots compared H2A.Z, acH2A.Z, and acH2A.Z/H2AZ with DNA methylation status in PrEC (*top*) and LNCaP cells (*bottom*). The average signal of corresponding ChIP-on-chip data (*y*-axis: signal intensity) of highly methylated genes (>80% relative to the SssI) is represented as a red line along the gene promoter (*x*-axis), whereas lowly methylated genes are represented as a black line (<20% relative to the SssI). Blue line represents randomly selected genes from the pool of neither high nor lowly methylated; light-blue background covers the 95% confidence interval of the data. (*B*) Significance plots for the average signal of H2A.Z, acH2A.Z, and acH2A.Z/H2A.Z along gene promoters that change in expression and DNA methylation in LNCaP compared with PrEC (LNCaP-PrEC). Red line corresponds to DNA hypermethylated (≥2-fold) and down-regulated (≥1.5 t-stats) genes; black line represents DNA hypomethylated (≤−2-fold) and down-regulated genes (≤−1.5 t-stats) in LNCaP-PrEC. (*C*) Three gene examples (*RND3, MKRN3*, and *LIMCH1*) that show change in acH2A.Z/H2A.Z promoter enrichment and DNA methylation in prostate cancer. ChIP qPCR of H2A.Z and acH2A.Z confirms a gain of acH2A.Z/H2A.Z. DNA methylation using Sequenom MALDI-TOF analysis of genomic DNA from the promoter region was calculated by averaging the ratios obtained from each CpG site from both LNCaP and PrEC. CpG sites correspond to the same regions analyzed for H2A.Z and acH2A.Z occupancy.

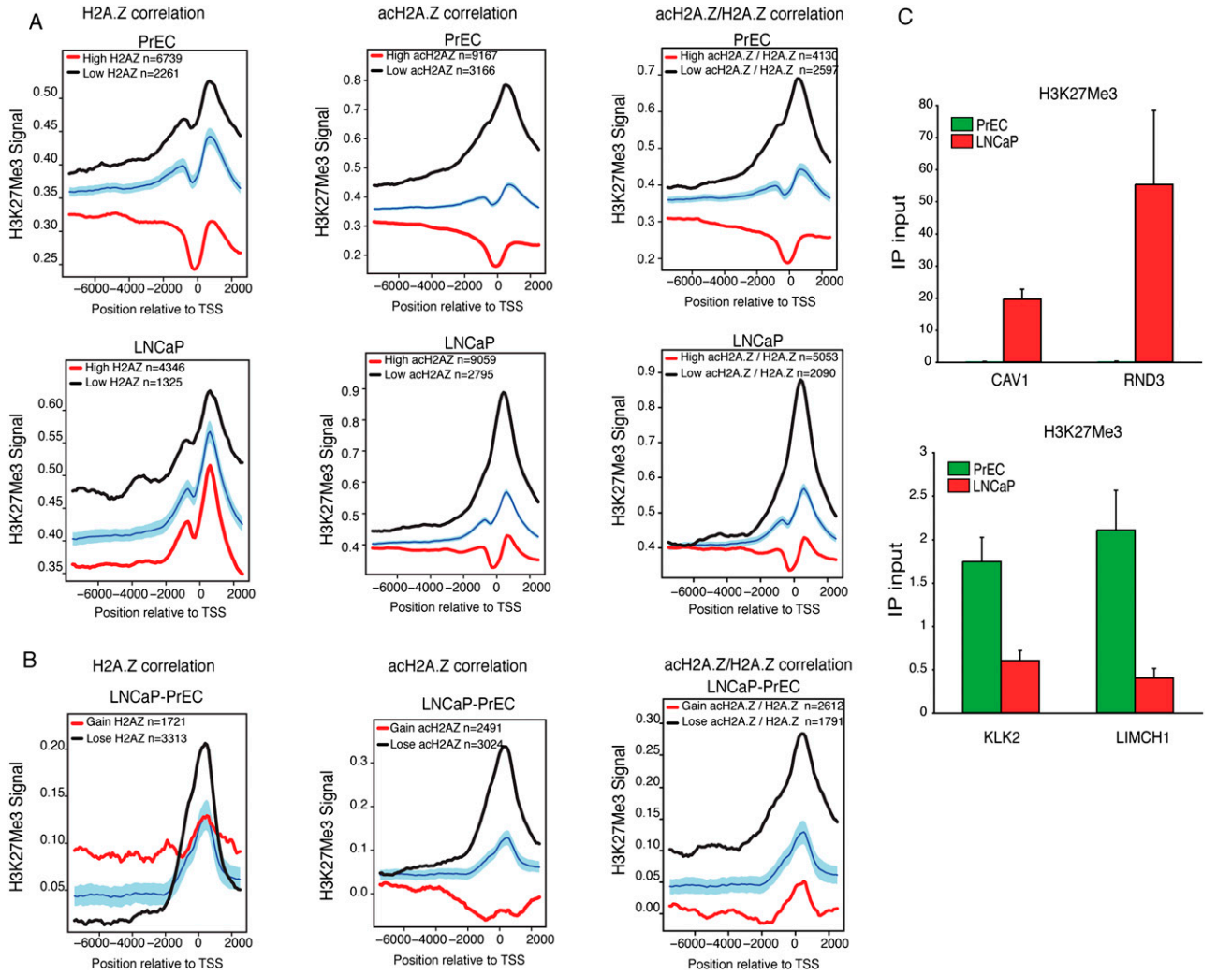

Figure 7. Anticorrelation between H3K27me3 and H2A.Z or acH2A.Z promoter presence in prostate cancer. (*A*) Significance plots of H3K27me3 signal comparing H2A.Z, acH2A.Z, and acH2A.Z/H2A.Z along gene promoters in genes sorted by high (red line) or low (black line) levels of H2A.Z, acH2A.Z, and acH2A.Z/H2A.Z in PrEC (*top*) and LNCaP (*bottom*). The selection criteria of H2A.Z, acH2A.Z, and acH2A.Z/H2A.Z for high levels were t-stats ≥ 1.5 (red line), and t-stats ≤ -1.5 for low levels (black line), as explained in the Supplemental Methods. (*B*) Significance plots of changes in the H3K27me3 signal (LNCaP-PrEC) along gene promoters in genes sorted by gain (t-stats ≥ 1.5, red line) or loss (t-stats ≤ -1.5, black line) of H2A.Z, acH2A.Z, and acH2A.Z/H2A.Z in LNCaP-PrEC. (*C*) ChIP qPCR using H3K27me3 antibody was performed to validate the anticorrelation in four different prostate cancer–related genes: *CAV1* and *RND3* (*top*) and *KLK2* and *LIMCH1* (*bottom*). See Figure 4 for validation of H2A.Z, acH2A.Z levels.

in promoters and changes in H2A.Z acetylation states, and that acetylation of H2A.Z could be a plausible target for prostate cancer management (Rangasamy 2010).

Acetylation of H2A.Z is anticorrelated with both DNA methylation and K27me3, and is prevalent in gene deregulation during carcinogenesis

The mutual exclusion between DNA methylation and H2A.Z deposition has been recently reported in mice (Conerly et al. 2010). Here, we find that it is primarily the acetylation of H2A.Z that is anticorrelated with DNA methylation. Moreover, we find that acH2A.Z anticorrelates with the presence of the repressive polycomb H3K27me3 mark. In fact, we demonstrate that alteration of H2A.Z acetylation in prostate cancer is associated with an inverse change in DNA methylation and/or H3K27me3 status. In embryonic stem cells, H2A.Z and polycomb protein occupancy is interdependent at promoters of developmentally important genes; however, this is not maintained in lineage-committed cells (Creyghton et al. 2008). Our data suggest the opposite pattern in prostate cells, where, in particular, the presence of acH2A.Z strongly anticorrelates with K27me3 mark.

Conclusion

We show that in mammals modification of H2A.Z by acetylation is the primary mark that mutually excludes DNA methylation and/or H3K27me3, rather than H2A.Z occupancy alone. We propose that acH2A.Z contributes to unstable nucleosomes, and in concert with DNA demethylation and/or loss of K27me3 promotes an unstable region to allow the access of the transcription machinery to activate gene expression. Conversely, gene repression is associated with deacetylation of H2A.Z at transcriptional start sites in com-

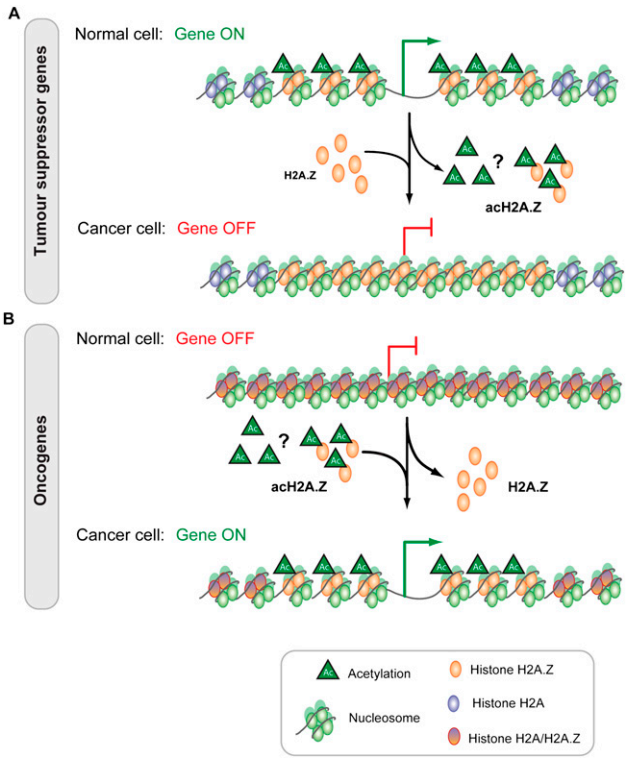

Figure 8. Model of gene transcriptional regulation dependent on H2A.Z occupancy and its acetylated state in prostate cancer. (*A*) In a normal cell, genes that are actively transcribed exhibit a bimodal distribution of at least three acetylated H2A.Z nucleosomes plus and minus the TSS. In cancer, some inactivated genes (including TSG), undergo epigenetic change across the promoter that includes deacetylation of H2A.Z nucleosomes, either through active deacetylation or exchange of a H2A.Z nucleosome (depicted as "?"). (*B*) In contrast, in a normal cell inactive genes contain a mix of H2A and H2A.Z nucleosomes across the entire promoter (H2A/H2A.Z nucleosomes). The apparent mix of H2A or H2A.Z–nucleosomes could be heterotypic nucleosomes containing one H2A dimer and one H2A.Z dimer, or H2A.Z and H2A homotypic nucleosomes deposited alternatively across the promoter. In a cancer cell there is a general loss of H2A.Z nucleosomes, together with a gain of acH2A.Z nucleosomes plus and minus three or more nucleosomes around the TSS, either through active acetylation or exchange of a H2A.Z nucleosome (depicted as "?"), resulting in an overexpression of these genes (e.g., oncogenes).

bination with promoter DNA hypermethylation and/or gain of H3K27me3. Further research is required to investigate what drives the prescriptive pattern of H2A.Z localization and what initiates H2A.Z acetylation associated with gene transcription in normal cells and its deregulation in cancer.

Methods

Cell lines and culture conditions

LNCaP, DU-145, and PC-3 prostate cancer cells and two independent cultures of normal prostate epithelial cells PrEC cells (Cambrex Bio Science Cat. No. CC-2555: $PrEC_1$ and $PrEC_2$; tissue acquisition nos. #13683 and #13639) were cultured as described previously (Coolen et al. 2010). LNCaP cells were treated with Trichostatin A (TSA; Sigma) at 100 nM for 48 h, adding fresh TSA every 24 h. LNCaP cells were also treated with Anacardic Acid (6-pentadecylsalicylic acid, AA; Calbiochem) at 90 μM for 48 h. The untreated controls were mock treated with the equivalent amount of the vehicle used to dissolve the drugs, 100% ethanol for the TSA experiments, and 100% DMSO for AA treatment.

RNA isolation and gene expression array analysis

RNA was extracted from cell lines using TRIzol reagent (Invitrogen) and Affymetrix GeneChip HuGene 1.0 ST were performed as described previously (Coolen et al. 2010). Analysis of expression array data is described in the Supplemental Methods.

Chromatin immunoprecipitation (ChIP) assays

The ChIP assays for acetylated-histone H3 (H3K9ac), K4 trimethyl-histone H3 (H4K4me3), and K27 trimethyl-histone H3 (H3K27me3) were performed previously (Coolen et al. 2010). H2A, H2A.Z, and acetylated H2A.Z (acH2A.Z) ChIP assays were carried out according to Coolen et al. (2010) using antibodies specific for H2A.Z (Abcam#ab4174), H3 (Abcam#: ab1791), H2A.Z acetyl K4+K7+K11 (Abcam#ab18262), and H2A (Abcam#ab18255). Note H2A.Z (Abcam#ab4174) antibody recognizes both acetylated and deacetylated forms, whereas H2A.Z acetyl K4+K7+K11 (Abcam#ab18262) only recognizes acH2AZ. See the Supplemental Methods for a detailed explanation.

Whole-genome amplification and promoter array analyses

Immunoprecipitated DNA and input DNA from ChIP was amplified with GenomePlex Complete Whole Genome Amplification (WGA) Kit (Sigma Cat. No.#WGA2) according to the manufacturer's instructions and hybridized to Affymetrix GeneChip Human Promoter 1.0R Array as described previously (Coolen et al. 2010). Analysis of arrays was performed as described in the Supplemental Methods using two independent IPs per biological sample, where the correlation coefficients were above 0.89. Enrichment of ChIP signals was visualized using the UCSC Genome Browser software (http://genome.ucsc.edu/).

Methylation profiling by MBD2 capture

The MethylMiner Methylated DNA Enrichment Kit (Invitrogen) was used to isolate methylated DNA from LNCaP and PrEC cell lines according to Nair et al. (2011) CpG Genome universal methylated DNA obtained from Millipore (Cat# 57821) was used for fully methylated positive control DNA. Bound methylated DNA was eluted in a single fraction using High Salt Elution Buffer (Nair et al. 2011) and resuspended in 60 uL of H_2O. Ten nanograms of MBD captured DNA were used for library preparation, and Illumina GAII sequencing was performed at the Ramaciotti Center, UNSW, Sydney to generate a 36-bp read length. The 36-bp reads were mapped to the hg18 reference genome using Bowtie (Langmead et al. 2009), with up to three mismatches. Reads that mapped more than once to a single genomic location were filtered. With one lane of Illumina Genome Analyzer sequencing with 36-base single end reads, we were able to uniquely map 10,491,054 and 10,139,044 for PrEC and LNCaP, respectively.

Quantitative real-time RT–PCR validation analysis of gene expression

RT–PCR analysis was performed as described previously (Frigola et al. 2006). Primers used for RT–PCR amplification (qPCR) are listed in Supplemental Table 5 and used as described previously for *CAV1* and *CAV2* (Coolen et al. 2010). Reactions were performed in triplicate, and standard deviation calculated using the $2^{-\Delta\Delta Ct}$ method (RQ) (Livak and Schmittgen 2001) (Applied Biosystems

User Bulletin N°2 [P/N 4303859]) to calculate the relative gene expression between LNCaP and PrEC cells. The data are presented as the fold change in mRNA gene expression of each gene normalized to either *GAPDH* or *ALAS1* as endogenous reference gene and relative to the normal cell line PrEC

Validation of ChIP–chip arrays by quantitative real-time PCR analysis

The amount of target immunoprecipitated was measured by qPCR using the ABI Prism 7900HT Sequence Detection System as described previously (Coolen et al. 2010). The amplification primers used for validation are listed in Supplemental Table 5. For each sample, the amount of material that was immunopreciptated relative to the amount of input chromatin was calculated according to Coolen et al. (2010). Experiments were repeated at least three times.

DNA methylation analysis using Sequenom analysis

DNA was extracted from cell lines using DNeasy Blood and Tissue Kit (QIAGEN) according to the manufacturer's instructions. Bisulphite treatment was carried out as previously described (Clark et al. 2006). As controls for the methylation analysis, whole-genome-amplified (WGA) DNA (0% methylated) and M.SssI-treated DNA (100% methylated) (Millipore#S7821) were bisulphite treated in parallel. Sequenom methylation analysis was performed as described previously (Coolen et al. 2007). The results were analyzed by the EpiTYPER software V 1.0 and methylation ratios were calculated as described in Nair et al. (2011).

Computational analyses for gene expression, tiling arrays, and MBDCap sequencing data comparisons

Heatmaps and line plots

For correlation analyses between gene expression and H2A, H2A.Z, acH2A.Z, H3K9ac, H3K4me3, and H3K27me3 binding, the "binPlots" procedure from the Repitools R package (Statham et al. 2010) was used. Briefly, the MAT-normalized tiling array data was smoothed using a trimmed mean over windows of 600 bases that contained 10 or more probes. Heatmaps or line plots were generated as summaries of these smoothed values over the regions of promoters (7500 bp upstream to 2450 bp downstream) where data is available. Genes were grouped according to summarized gene expression levels (see Supplemental Methods) and median-smoothed tiling array signal was calculated for each group and each region of the promoter.

Box plots and gene set tests

Box plots showing the distribution of t-statistics (See Supplemental Methods) for changes in H2A.Z, acH2A.Z, and acH2A.Z/H2A.Z (between LNCaP and PrEC) were made to interrogate the cross-talk between acH2A.Z and H2A.Z in deregulated genes. The top 10% of down-regulated genes that have a acH2A.Z/H2A.Z t-stats value ≤ -1.5 were selected as the group of "down-regulated genes + loss of acH2A.Z/H2A.Z" (479 genes in total); for "up-regulated genes + gain of acH2A.Z/H2A.Z", the top 10% of up-regulated genes that have a acH2A.Z/H2A.Z t-stats value ≥ 1.5 were extracted (545 genes in total). For testing the changes in signal for gene sets as a whole, the null distribution contains t-statistics of all genes that did not belong to either the down-regulated category or the up-regulated category. The *P*-values of the significance of differences between groups of genes were obtained with the "geneSetTest" in the R *limma* package (Smyth 2004).

Gene set profile plots

Plots of tiling array signal (H2A.Z, acH2A.Z, acH2A.Z/H2A.Z, and K27Me3) and MBDCap across the promoter summarized over gene sets of interest, so-called gene-set profile plots, were created using the "significancePlots" procedure in the Repitools R package (Statham et al. 2010). Briefly, the smoothed tiling array signal is summarized for probes at each region of the promoter. To create a basis for comparison, many random gene sets (of the size of the biggest gene set) are taken and 2.5%-ile, 50%-ile (median), and 97.5%-iles of signal are plotted. The gene sets selected are explained in the Supplemental Methods.

Data access

Data from this study have been submitted to the NCBI Gene Expression Omnibus (http://ncbi.nlm.nih.gov/geo) under SuperSeries accession numbers GSE25914, GSE24546, and GSE19726.

Acknowledgments

This work is supported by a National Health and Medical Research Council (NH&MRC) Fellowship (S.J.C.) and the Prostate Cancer Foundation of Australia (PCFA). We thank the Ramaciotti Centre, University of NSW (Sydney, Australia) for array hybridizations and Illumina GAII sequencing of MBDCap DNA.

References

Balasubramanyam K, Swaminathan V, Ranganathan A, Kundu TK. 2003. Small molecule modulators of histone acetyltransferase p300. *J Biol Chem* **278:** 19134–19140.

Barski A, Cuddapah S, Cui K, Roh TY, Schones DE, Wang Z, Wei G, Chepelev I, Zhao K. 2007. High-resolution profiling of histone methylations in the human genome. *Cell* **129:** 823–837.

Bernstein BE, Kamal M, Lindblad-Toh K, Bekiranov S, Bailey DK, Huebert DJ, McMahon S, Karlsson EK, Kulbokas EJ 3rd, Gingeras TR, et al. 2005. Genomic maps and comparative analysis of histone modifications in human and mouse. *Cell* **120:** 169–181.

Bruce K, Myers FA, Mantouvalou E, Lefevre P, Greaves I, Bonifer C, Tremethick DJ, Thorne AW, Crane-Robinson C. 2005. The replacement histone H2A.Z in a hyperacetylated form is a feature of active genes in the chicken. *Nucleic Acids Res* **33:** 5633–5639.

Campos EI, Reinberg D. 2009. Histones: annotating chromatin. *Annu Rev Genet* **43:** 559–599.

Chakravarthy S, Bao Y, Roberts VA, Tremethick D, Luger K. 2004. Structural characterization of histone H2A variants. *Cold Spring Harb Symp Quant Biol* **69:** 227–234.

Clark SJ, Statham A, Stirzaker C, Molloy PL, Frommer M. 2006. DNA methylation: bisulphite modification and analysis. *Nat Protoc* **1:** 2353–2364.

Conerly ML, Teves SS, Diolaiti D, Ulrich M, Eisenman RN, Henikoff S. 2010. Changes in H2A.Z occupancy and DNA methylation during B-cell lymphomagenesis. *Genome Res* **20:** 1383–1390.

Coolen MW, Statham AL, Gardiner-Garden M, Clark SJ. 2007. Genomic profiling of CpG methylation and allelic specificity using quantitative high-throughput mass spectrometry: critical evaluation and improvements. *Nucleic Acids Res* **35:** e119. doi: 10.1093/nar/gkm662.

Coolen MW, Stirzaker C, Song JZ, Statham AL, Kassir Z, Moreno CS, Young AN, Varma V, Speed TP, Cowley M, et al. 2010. Consolidation of the cancer genome into domains of repressive chromatin by long-range epigenetic silencing (LRES) reduces transcriptional plasticity. *Nat Cell Biol* **12:** 235–246.

Creyghton MP, Markoulaki S, Levine SS, Hanna J, Lodato MA, Sha K, Young RA, Jaenisch R, Boyer LA. 2008. H2AZ is enriched at polycomb complex target genes in ES cells and is necessary for lineage commitment. *Cell* **135:** 649–661.

Dhillon N, Oki M, Szyjka SJ, Aparicio OM, Kamakaka RT. 2006. H2A.Z functions to regulate progression through the cell cycle. *Mol Cell Biol* **26:** 489–501.

Dion MF, Kaplan T, Kim M, Buratowski S, Friedman N, Rando OJ. 2007. Dynamics of replication-independent histone turnover in budding yeast. *Science* **315:** 1405–1408.

Doyon Y, Cote J. 2004. The highly conserved and multifunctional NuA4 HAT complex. *Curr Opin Genet Dev* **14:** 147–154.
Dunican DS, McWilliam P, Tighe O, Parle-McDermott A, Croke DT. 2002. Gene expression differences between the microsatellite instability (MIN) and chromosomal instability (CIN) phenotypes in colorectal cancer revealed by high-density cDNA array hybridization. *Oncogene* **21:** 3253–3257.
Faast R, Thonglairoam V, Schulz TC, Beall J, Wells JR, Taylor H, Matthaei K, Rathjen PD, Tremethick DJ, Lyons I. 2001. Histone variant H2A.Z is required for early mammalian development. *Curr Biol* **11:** 1183–1187.
Frigola J, Song J, Stirzaker C, Hinshelwood RA, Peinado MA, Clark SJ. 2006. Epigenetic remodeling in colorectal cancer results in coordinate gene suppression across an entire chromosome band. *Nat Genet* **38:** 540–549.
Futreal PA, Coin L, Marshall M, Down T, Hubbard T, Wooster R, Rahman N, Stratton MR. 2004. A census of human cancer genes. *Nat Rev Cancer* **4:** 177–183.
Gevry N, Chan HM, Laflamme L, Livingston DM, Gaudreau L. 2007. p21 transcription is regulated by differential localization of histone H2A.Z. *Genes Dev* **21:** 1869–1881.
Gevry N, Hardy S, Jacques PE, Laflamme L, Svotelis A, Robert F, Gaudreau L. 2009a. Histone H2A.Z is essential for estrogen receptor signaling. *Genes Dev* **23:** 1522–1533.
Gevry N, Hardy S, Jacques PE, Laflamme L, Svotelis A, Robert F, Gaudreau L. 2009b. Histone H2A.Z is essential for estrogen receptor signaling. *Genes Dev* **23:** 1522–1533.
Greaves IK, Rangasamy D, Ridgway P, Tremethick DJ. 2007. H2A.Z contributes to the unique 3D structure of the centromere. *Proc Natl Acad Sci* **104:** 525–530.
Guillemette B, Gaudreau L. 2006. Reuniting the contrasting functions of H2A.Z. *Biochem Cell Biol* **84:** 528–535.
Halley JE, Kaplan T, Wang AY, Kobor MS, Rine J. 2010. Roles for H2A.Z and its acetylation in GAL1 transcription and gene induction, but not GAL1-transcriptional memory. *PLoS Biol* **8:** e1000401. doi: 10.1371/journal.pbio.1000401.
Hardy S, Jacques PE, Gevry N, Forest A, Fortin ME, Laflamme L, Gaudreau L, Robert F. 2009. The euchromatic and heterochromatic landscapes are shaped by antagonizing effects of transcription on H2A.Z deposition. *PLoS Genet* **5:** e1000687. doi: 10.1371/journal.pgen.1000687.
Higgins ME, Claremont M, Major JE, Sander C, Lash AE. 2007. CancerGenes: a gene selection resource for cancer genome projects. *Nucleic Acids Res* **35:** D721–D726.
Hua S, Kallen CB, Dhar R, Baquero MT, Mason CE, Russell BA, Shah PK, Liu J, Khramtsov A, Tretiakova MS, et al. 2008. Genomic analysis of estrogen cascade reveals histone variant H2A.Z associated with breast cancer progression. *Mol Syst Biol* **4:** 188. doi: 10.1038/msb.2008.25.
Ishibashi T, Dryhurst D, Rose KL, Shabanowitz J, Hunt DF, Ausio J. 2009. Acetylation of vertebrate H2A.Z and its effect on the structure of the nucleosome. *Biochemistry (Mosc)* **48:** 5007–5017.
Kamakaka RT, Biggins S. 2005. Histone variants: deviants? *Genes Dev* **19:** 295–310.
Langmead B, Trapnell C, Pop M, Salzberg SL. 2009. Ultrafast and memory-efficient alignment of short DNA sequences to the human genome. *Genome Biol* **10:** R25. doi: 10.1186/gb-2009-10-3-r25.
Livak KJ, Schmittgen TD. 2001. Analysis of relative gene expression data using real-time quantitative PCR and the 2(-Delta Delta C(T)) Method. *Methods* **25:** 402–408.
Lu PY, Levesque N, Kobor MS. 2009. NuA4 and SWR1-C: two chromatin-modifying complexes with overlapping functions and components. *Biochem Cell Biol* **87:** 799–815.
Marques M, Laflamme L, Gervais AL, Gaudreau L. 2010. Reconciling the positive and negative roles of histone H2A.Z in gene transcription. *Epigenetics* **5:** 267–272.
Millar CB, Xu F, Zhang K, Grunstein M. 2006. Acetylation of H2AZ Lys 14 is associated with genome-wide gene activity in yeast. *Genes Dev* **20:** 711–722.
Mizuguchi G, Shen X, Landry J, Wu WH, Sen S, Wu C. 2004. ATP-driven exchange of histone H2AZ variant catalyzed by SWR1 chromatin remodeling complex. *Science* **303:** 343–348.
Nair SS, Coolen MW, Stirzaker C, Song JZ, Statham AL, Strbenac D, Robinson MD, Clark SJ. 2011. Comparison of methyl-DNA immunoprecipitation (MeDIP) and methyl-CpG binding domain (MBD) protein capture for genome-wide DNA methylation analysis reveal CpG sequence coverage bias. *Epigenetics* **6:** 34–44.
Ozsolak F, Song JS, Liu XS, Fisher DE. 2007. High-throughput mapping of the chromatin structure of human promoters. *Nat Biotechnol* **25:** 244–248.
Rangasamy D. 2010. Histone variant H2A.Z can serve as a new target for breast cancer therapy. *Curr Med Chem* **17:** 3155–3161.
Rangasamy D, Berven L, Ridgway P, Tremethick DJ. 2003. Pericentric heterochromatin becomes enriched with H2A.Z during early mammalian development. *EMBO J* **22:** 1599–1607.
Rangasamy D, Greaves I, Tremethick DJ. 2004. RNA interference demonstrates a novel role for H2A.Z in chromosome segregation. *Nat Struct Mol Biol* **11:** 650–655.
Ren Q, Gorovsky MA. 2001. Histone H2A.Z acetylation modulates an essential charge patch. *Mol Cell* **7:** 1329–1335.
Rhodes DR, Yu J, Shanker K, Deshpande N, Varambally R, Ghosh D, Barrette T, Pandey A, Chinnaiyan AM. 2004. Large-scale meta-analysis of cancer microarray data identifies common transcriptional profiles of neoplastic transformation and progression. *Proc Natl Acad Sci* **101:** 9309–9314.
Rong YS. 2008. Loss of the histone variant H2A.Z restores capping to checkpoint-defective telomeres in *Drosophila*. *Genetics* **180:** 1869–1875.
Santisteban MS, Kalashnikova T, Smith MM. 2000. Histone H2A.Z regulates transcription and is partially redundant with nucleosome remodeling complexes. *Cell* **103:** 411–422.
Sarcinella E, Zuzarte PC, Lau PN, Draker R, Cheung P. 2007. Monoubiquitylation of H2A.Z distinguishes its association with euchromatin or facultative heterochromatin. *Mol Cell Biol* **27:** 6457–6468.
Schones DE, Cui K, Cuddapah S, Roh TY, Barski A, Wang Z, Wei G, Zhao K. 2008. Dynamic regulation of nucleosome positioning in the human genome. *Cell* **132:** 887–898.
Sharma S, Kelly TK, Jones PA. 2010. Epigenetics in cancer. *Carcinogenesis* **31:** 27–36.
Smyth GK. 2004. Linear models and empirical bayes methods for assessing differential expression in microarray experiments. *Stat Appl Genet Mol Biol* **3:** doi: 10.2202/1544-6115.1027.
Statham AL, Strbenac D, Coolen MW, Stirzaker C, Clark SJ, Robinson MD. 2010. Repitools: an R package for the analysis of enrichment-based epigenomic data. *Bioinformatics* **26:** 1662–1663.
Sutcliffe EL, Parish IA, He YQ, Juelich T, Tierney ML, Rangasamy D, Milburn PJ, Parish CR, Tremethick DJ, Rao S. 2009. Dynamic histone variant exchange accompanies gene induction in T cells. *Mol Cell Biol* **29:** 1972–1986.
Suto RK, Clarkson MJ, Tremethick DJ, Luger K. 2000. Crystal structure of a nucleosome core particle containing the variant histone H2A.Z. *Nat Struct Biol* **7:** 1121–1124.
Viens A, Mechold U, Brouillard F, Gilbert C, Leclerc P, Ogryzko V. 2006. Analysis of human histone H2AZ deposition in vivo argues against its direct role in epigenetic templating mechanisms. *Mol Cell Biol* **26:** 5325–5335.
Weber CM, Henikoff JG, Henikoff S. 2010. H2A.Z nucleosomes enriched over active genes are homotypic. *Nat Struct Mol Biol* **17:** 1500–1507.
Wolff EM, Byun HM, Han HF, Sharma S, Nichols PW, Siegmund KD, Yang AS, Jones PA, Liang G. 2010. Hypomethylation of a LINE-1 promoter activates an alternate transcript of the MET oncogene in bladders with cancer. *PLoS Genet* **6:** e1000917. doi: 10.1371/journal.pgen.1000917.
Zemach A, McDaniel IE, Silva P, Zilberman D. 2010. Genome-wide evolutionary analysis of eukaryotic DNA methylation. *Science* **328:** 916–919.
Zilberman D, Coleman-Derr D, Ballinger T, Henikoff S. 2008. Histone H2A.Z and DNA methylation are mutually antagonistic chromatin marks. *Nature* **456:** 125–129.
Zlatanova J, Thakar A. 2008. H2A.Z: view from the top. *Structure* **16:** 166–179.
Zofall M, Fischer T, Zhang K, Zhou M, Cui B, Veenstra TD, Grewal SI. 2009. Histone H2A.Z cooperates with RNAi and heterochromatin factors to suppress antisense RNAs. *Nature* **461:** 419–422.
Zucchi I, Mento E, Kuznetsov VA, Scotti M, Valsecchi V, Simionati B, Vicinanza E, Valle G, Pilotti S, Reinbold R, et al. 2004. Gene expression profiles of epithelial cells microscopically isolated from a breast-invasive ductal carcinoma and a nodal metastasis. *Proc Natl Acad Sci* **101:** 18147–18152.

Received December 7, 2010; accepted in revised form June 7, 2011.